Fabrication of on-chip photo lantern for vertical coupling of multimode optic fiber to silicon oxynitride waveguide

Xiaobin Cui [1], Shengfeng Deng [2], Miao Lu [2], *

[1]Department of Mechanical and Electrical Engineering, Xiamen University, China

[2]Pen-Tung Sah Institute of Micro-Nano Science & Technology, Xiamen University, China

*lm@xmu.edu.cn

Abstract. Spectroscopy is a powerful tool for identifying chemicals in environment, food and industry etc. Chip spectrometer will boost the application of spectroscopy because it is portable and able to be produced in batch with low cost. However, the coupling between multimode fiber and waveguide was a significant obstacle in the realization of chip spectrometer. An on-chip photo lantern was proposed in this paper to convert the multimode light into multi-channels single mode light, and couple to a chip spectrometer vertically. The design, simulation and fabrication of the on-chip photo lantern were introduced. The proposed technology is promising for improving the sensitivity of chip spectrometer.

Keywords: multimode fiber to waveguide coupling; chip spectrometer; on-chip photo lantern.

1. Introduction

The coupling of single-mode optic fiber to waveguide is well developed in the past 30 years due to the huge demand comes from optical communication and optical interconnection [1-5]. However, multimode fiber with a core size large than 100 micron is normally used to collect enough scattering light in a fiber spectroscopy system. In recent, with the development of on-chip spectrometer [6-16], efficient multimode fiber-waveguide coupling techniques are in demand. Since the diameter of the output light spot of multimode fiber is normally more than a hundred micron while the core size of waveguide is only several micron, a large coupling loss is normally unavoidable in a horizontal direct coupling mode because of the large core size mismatch. Accordingly, many researches focused on the development of vertically coupling techniques. Although the grating coupling technology of single mode fiber-waveguide is well developed [17-26], the vertically coupling of multimode fiber-waveguide faced more difficulties due to mode conversion and is far from usable. For example, it is difficult to calculate the spatial distribution of multimode light as well as its emission angle using electromagnetic theory because the theoretical analysis on so many modes is too complex to be accomplished. It is almost impossible to establish a theoretical model on coupling of multimode fiber to waveguide. The experimental coupling efficiency of multimode fiber to waveguide is also poor due to the mode mismatch.

A feasible solution is to convert multimode light into multichannel single mode light firstly, and then couple into waveguide vertically. An optical component called photo lantern had been reported to covert multimode light to an array of single mode light [27-34]. One end of a photo lantern is a multimode fiber while the other end is a bundle of single mode fibers. The contour of these single mode fibers formed a circle with the diameter that equals to the core size of the multimode fiber.

A vertically multimode fiber-waveguide coupling approach was introduced in this paper for the application on an on-chip spectrometer. A tilted polymeric pillar array was fabricated on a taper silicon oxynitride waveguide, and the diameter of each pillar was limited to a few micron to allow only single mode transmission. These pillars were arranged close to each other and the silicon substrate under these pillars was removed and a metal reflective layer was then deposited. In the on-chip spectrometer, the input multimode fiber was fixed on the top of these pillars, and the multimode light was covert into many isolated single-mode beams along these pillars and further coupling into the taper waveguide. The design, simulation, fabrication and testing of the coupling structure was discussed in the following sections.

2. Theoretical Analysis and Simulation

The cross section of the proposed on-chip photo lantern was illustrated in Fig.1. The refractive index of cladding and core layer of oxynitride waveguide are 1.454 and 1.483, respectively. The thickness of core layer is about 1.5 micron to allow the transmission of only single mode light. The thickness of top and bottom cladding layer is about 4 micron. The vertical polymeric waveguide is formed by SU-8 photo resist and its refractive index is 1.574. α and c is the angle of total reflection of the oxynitride waveguide and SU-8 vertical waveguide, respectively. β is the refractive angle from SU-8 to oxynitride core layer. The following equations can then be derived according to the classical optical theory.

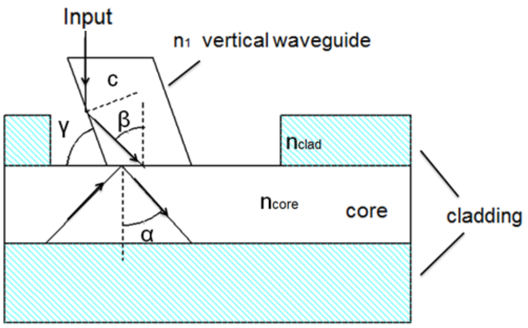

Figure1 The model of vertical coupling with titling polymeric pillar

$$\frac{\sin\alpha}{\sin\beta} = \frac{n_1}{n_{core}} \quad (1)$$

$$\sin c = \frac{n_{air}}{n_1} \quad (2)$$

$$\sin\alpha = \frac{n_{clad}}{n_{core}} \quad (3)$$

Where n_{air} is the refractive index of air. We can derive the solution of these equations by substitute the value of n_1, n_{air}, n_{core} and n_{clad} into equation 1-3. The solution of these equations are c=39.6˚, α=78.6˚, β=67.8˚. The incline angle of the SU-8 vertical waveguide is determined to be γ=72.6°.

Simulation was carried out using the software FDTD based on the model shown in Fig. 1.The simulated result was shown in Fig. 2. Here the input light irradiation on the top surface of the on-chip photo lantern vertically and coupled into the core layer of the underneath oxynitride waveguide. The coupling efficiency is defined as the ratio of output and input optical power.

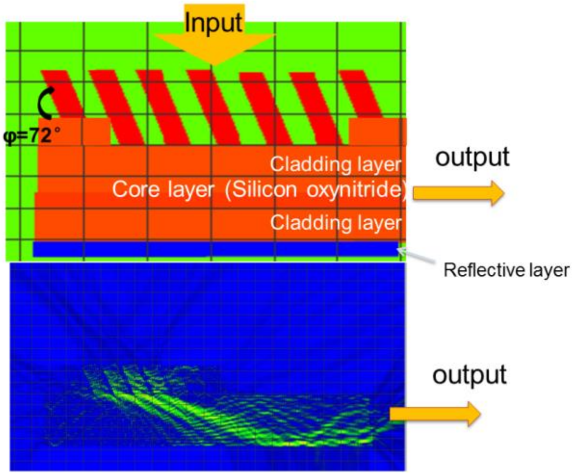

Figure 2 Simulation model and result of vertical coupling structure by FDTD

The diameter of the SU-8 pillar as well as the gap between adjacent pillars was determined by the minimum size allowed by the lithography process in our lab. The height of the SU-8 pillar was optimized by maximizing the efficiency and reducing the difference of efficiency from 800-1000 nm, which is the range of Raman chip spectrometer with a 785 nm irradiation laser. The simulated efficiency was shown in Fig. 3 with the height of SU-8 pillar ranged from 4.3 to 5.0 micron. Finally, the diameter of SU-8 pillar is 2.0 micron while their gap is 2.0 micron, too. The height of SU-8 pillar is determined to be 4.9 micron.

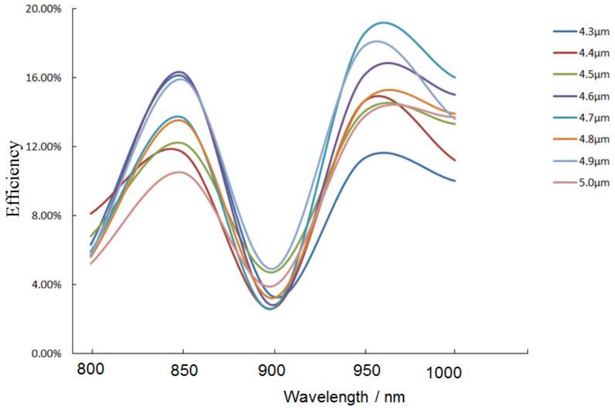

Figure 3 The coupling efficiency with different height of SU-8 pillars

3. Fabrication

3.1 Fabrication of photomask by direct laser writing

The collimated ultraviolent light should irradiate the wafer in an incline angle in order to realize a tilting SU-8 pillar array in the exposure process. A feasible way is to place the wafer as well as its photomask on a leaned base. However, the commercial available photomask is too bulky to be amounted on a leaned base. We made a compact photomask instead by direct laser writing.

Chrome 200 nm thick was sputtered on a glass wafer about 400 micron thick. A photo resist (AZ 1805, Shipley) was spin-coated at 7000 rpm for 30 second and prebaked at 95 C for 4 minutes. The wafer was developed for 1 minutes using a TMAH developer (RZX-3038, Ruihong Inc., China) after exposure using a laser direct writing system (Micro Writer MLTM, Quantum design Inc., Britain) at a dose of 9 mJ/cm^2. Then the wafer was immersed in a Chrome etching solution (NH4NO3: HClO4: H2O=100g: 26ml: 440ml) for 1 minute. The AZ 1805 photo resist was stripped by acetone and IPA. The glass was then diced to small pieces about 2 × 2 cm. Last, the photomask was rinsed by DI water and blow dry by nitrogen. The optical microscopy picture of the fabricated photomask was shown in Fig. 4

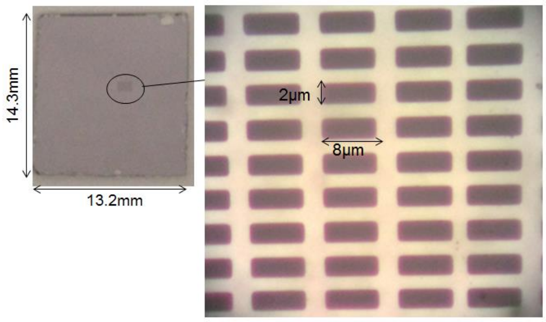

Figure 4 the OM pictures of fabricated photo mask by laser direct writing

3.2 Fabrication of Tilting SU-8 Pillar Array

The inclined base for the exposure of titling SU-8 pillar array was shown in Fig. 5. Because the size and gap of SU-8 pillars is only a few microns, it is essential to minimize the gap between the wafer and photomask to prevent the blurring of the photo resist pattern induced by UV diffraction. Two silica gel gaskets hold by trip bolts were placed on the pair of wafer and photo mask and pressed them together.

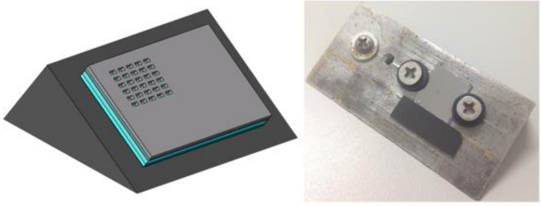

Figure 5 the illustration and the optical picture of the incline base

The inclined base for the exposure of titling SU-8 pillar array was shown in Fig. 5. Because the size and gap of SU-8 pillars is only a few microns, it is essential to minimize the gap between the wafer and photo mask to prevent the blurring of the photo resist pattern induced by diffraction. Two silica gel gaskets screwed by trip bolts was placed on the edge of the pair of wafer and photo mask and pressed them together tightly. DI water was dipped on the pair of wafer and photo mask to further reduce the effect of diffraction. The optical microscopy picture of the achieved SU-8 pillar array with or without water immersion were shown in Fig. 6. The lithograph resolution was improved significantly.

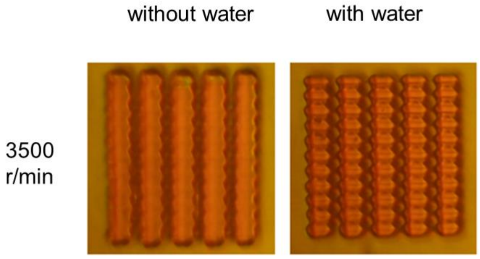

Fig.6 The OM picture of SU-8 pillars with or without water immersion

SU-8 2005 was spin-coated on a spectrometer chip at 3500 rpm for 30 second. The chip was placed on the inclined base after prebake at 65 C for 5 minutes and 95 C for another 5 minutes. The photo mask was placed on the chip face to face and pressed tightly by the silica gel gaskets as shown in Fig. 5. A dip of DI water was dipped on the edge of the pair of chip and photo mask. The DI water filled the gap between the chip and photo mask by capillary action. The inclined base was then moved to an contact aligner (BA6, Karlsuss, Germany) and exposed at a dose of 150 mJ/cm^2. The chip was developed for 3 minutes after bake at 65 C for 5 minutes and 95 C for another 5 minutes. Last, the chip was rinsed by IPA and blow dry by Nitrogen. The SEM picture of the fabricated SU-8 pillar array was shown in Fig. 7

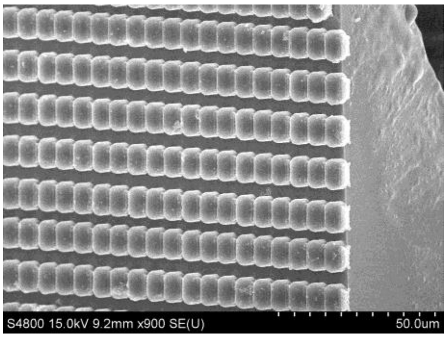

Figure 7 The SEM picture of fabricated titling SU-8 pillars

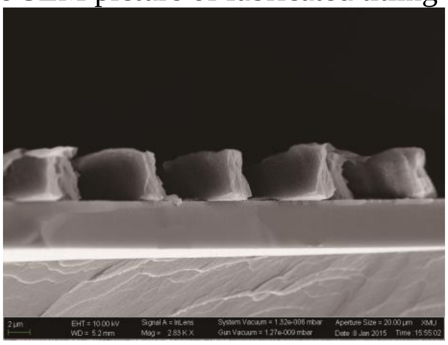

Figure 8 The SEM picture of the cross section of the on-chip photo lantern

As shown in Fig.1, A reflection layer under the oxynitride waveguide is required to improve the coupling efficiency. To prepare the reflection layer, the silicon substrate underneath the SU-8 pillar array was removed by wet etching and Aluminum 100 nm thick was then deposited on the backside of the chip. The SEM picture of cross section of the coupling structure was shown in Figure 8.

4. Conclusions

An vertically coupling approach of multimode fiber to oxynitride waveguide was investigated in this paper for the application of chip spectrometer. multimode light was converted to an array of single mode light by passing through a titling SU-8 pillars array, and coupling to oxynitride waveguide vertically. The fabrication process of the on-chip photo lantern was demonstrated. The optical characterization and the optimization of structural parameters is on-going and will be presented in a future paper.

Acknowledgments

This work was supported by NSFC under the project no. 21127001 and supported by the Fundamental Research Funds for the Central Universities under the project no. 2011121025.

Reference

[1] Mitomi O, Kasaya K, Miyazawa H. Design of a single-mode tapered waveguide for low-loss chip-to-fiber coupling[J]. Quantum Electronics, IEEE Journal of, 1994, 30(8): 1787-1793.
[2] Markov P, Valentine J G, Weiss S M. Fiber-to-chip coupler designed using an optical transformation[J]. Optics express, 2012, 20(13): 14705-14713.
[3] Alder T, Stohr A, Heinzelmann R, et al. High-efficiency fiber-to-chip coupling using low-loss tapered single-mode fiber[J]. Photonics Technology Letters, IEEE, 2000, 12(8): 1016-1018.
[4] Kasaya K, Mitomi O, Naganuma M, et al. A simple laterally tapered waveguide for low-loss coupling to single-mode fibers[J]. Photonics Technology Letters, IEEE, 1993, 5(3): 345-347.
[5] Hsu H P, Milton A F. Flip-chip approach to endfire coupling between single-mode optical fibres and channel waveguides[J]. Electronics Letters, 1976, 12(16): 404-405.
[6] Cheben P, Schmid J H, Delâge A, et al. A high-resolution silicon-on-insulator arrayed waveguide grating microspectrometer with sub-micrometer aperture waveguides[J]. Optics Express. 2007, 15(5): 2299-2306.
[7] Kodate K, Komai Y. Compact spectroscopic sensor using an arrayed waveguide grating[J]. Journal of Optics A: Pure and Applied Optics. 2008, 10(4): 44011.
[8] Kodate K, Komai Y, Okamoto K. Compact Spectroscopic Sensor Using an Arrayed Waveguide Grating[C]. IEEE, 2007.
[9] Komai Y, Nagano H, Okamoto K, et al. Compact spectroscopic sensor using a visible arrayed waveguide grating[J]. Japanese journal of applied physics. 2006, 45: 6742.
[10] Ismail N, Baclig A C, Caspers P J, et al. Design of low-loss arrayed waveguide gratings for applications in integrated Raman spectroscopy[C]. Optical Society of America, 2010.
[11] Ismail N, Choo-Smith L, Wörhoff K, et al. Raman spectroscopy with an integrated arrayed-waveguide grating[J]. Optics letters. 2011, 36(23): 4629-4631.
[12] Yebo N A, Bogaerts W, Hens Z, et al. On-chip arrayed waveguide grating interrogated silicon-on-insulator microring resonator-based gas sensor[J]. Photonics Technology Letters, IEEE. 2011, 23(20): 1505-1507.
[13] Sugita A, Kaneko A, Okamoto K, et al. Very low insertion loss arrayed-waveguide grating with vertically tapered waveguides[J]. Photonics Technology Letters, IEEE. 2000, 12(9): 1180-1182.
[14] Maru K, Chiba T, Okawa M, et al. Low-loss arrayed-waveguide grating with high index regions at slab-to-array interface[J]. Electronics Letters. 2001, 37(21): 1287-1289.
[15] Lu H, Wang W. Cyclic arrayed waveguide grating devices with flat-top passband and uniform spectral response[J]. Photonics Technology Letters, IEEE. 2008, 20(1): 3-5.

[16] Sakamaki Y, Kamei S, Hashimoto T, et al. Loss uniformity improvement of arrayed-waveguide grating with mode-field converters designed by wavefront matching method[J]. Lightwave Technology, Journal of. 2009, 27(24): 5710-5715.
[17] ZAOUI W S, KUNZE A, VOGEL W, et al. Bridging the gap between optical fibers and silicon photonic integrated circuits [J]. Optics Express, 2014, 22(2): 1277-86.
[18] CHENG Z, CHEN X, YAN WONG C, et al. Broadband focusing grating couplers for suspended-membrane waveguides [J]. Optics letters, 2012, 37(24): 5181-3.
[19] XU X, SUBBARAMAN H, COVEY J, et al. Complementary metal–oxide–semiconductor compatible high efficiency subwavelength grating couplers for silicon integrated photonics [J]. Applied Physics Letters, 2012, 101(3): 031109.
[20] HALIR R, CHEBEN P, SCHMID J, et al. Continuously apodized fiber-to-chip surface grating coupler with refractive index engineered subwavelength structure [J]. Optics letters, 2010, 35(19): 3243-5.
[21] SUBBARAMAN H, XU X, COVEY J, et al. Efficient light coupling into in-plane semiconductor nanomembrane photonic devices utilizing a sub-wavelength grating coupler [J]. Optics express, 2012, 20(18): 20659-65.
[22] QIN K, GAO D, BAO C, et al. High efficiency and broadband two-dimensional blazed grating coupler with fully etched triangular holes [J]. Journal of Lightwave Technology, 2012, 30(14): 2363-6.
[23] CHENG Z, CHEN X, WONG C, et al. Mid-infrared grating couplers for silicon-on-sapphire waveguides [J]. Photonics Journal, IEEE, 2012, 4(1): 104-13.
[24] ALONSO-RAMOS C, ZAVARGO-PECHE L, ORTEGA-MO UX A, et al. Polarization-independent grating coupler for micrometric silicon rib waveguides [J]. Optics letters, 2012, 37(17): 3663-5.
[25] CHEN X, TSANG H K. Polarization-independent grating couplers for silicon-on-insulator nanophotonic waveguides [J]. Optics letters, 2011, 36(6): 796-8.
[26] HALIR R, ORTEGA-MONUX A, SCHMID J H, et al. Recent advances in silicon waveguide devices using sub-wavelength gratings [J]. 2013,
[27] BLAND-HAWTHORN J, LAWRENCE J, ROBERTSON G, et al. PIMMS: photonic integrated multimode microspectrograph; proceedings of the SPIE Astronomical Telescopes+ Instrumentation, F, 2010 [C]. International Society for Optics and Photonics.
[28] NOORDEGRAAF D, SKOVGAARD P M, SANDBERG R, et al. Nineteen-port photonic lantern with multimode delivery fiber [J]. Optics letters, 2012, 37(4): 452-4.
[29] NOORDEGRAAF D, SKOVGAARD P M, MAACK M D, et al. Multi-mode to single-mode conversion in a 61 port Photonic Lantern [J]. Optics express, 2010, 18(5): 4673-8.
[30] FONTAINE N K, LEON-SAVAL S G, RYF R, et al. Mode-selective dissimilar fiber photonic-lantern spatial multiplexers for few-mode fiber; proceedings of the Proceedings of European Conference on Optical Communication, F, 2013 [C].
[31] LEON-SAVAL S G, FONTAINE N K, SALAZAR-GIL J R, et al. Mode-selective photonic lanterns for space-division multiplexing [J]. Optics express, 2014, 22(1): 1036-44.
[32] NOORDEGRAAF D, SKOVGAARD P M, NIELSEN M D, et al. Efficient multi-mode to single-mode coupling in a photonic lantern [J]. Optics Express, 2009, 17(3): 1988-94.
[33] RYF R, FONTAINE N K, MONTOLIU M, et al. Photonic-lantern-based mode multiplexers for few-mode-fiber transmission; proceedings of the Optical Fiber Communication Conference, F, 2014 [C]. Optical Society of America.
[34] HUANG B, FONTAINE N K, RYF R, et al. All-fiber mode-group-selective photonic lantern using graded-index multimode fibers [J]. Optics Express, 2015, 23(1): 224-34.